ISSN 1063-7826, Semiconductors, 2009, Vol. 43, No. 6, pp. 745–750. © Pleiades Publishing, Ltd., 2009.
Original Russian Text © O.Ya. Olikh, 2009, published in Fizika i Tekhnika Poluprovodnikov, 2009, Vol. 43, No. 6, pp. 774–779.

## ELECTRICAL AND OPTICAL PROPERTIES OF SEMICONDUCTORS

# The Variation in Activity of Recombination Centers in Silicon *p–n* Structures under the Conditions of Acoustic Loading

**O. Ya. Olikh**

*Physical Faculty, Kiev National University, ul. Vladimirskaya 64, Kiev, 03127 Ukraine*
*e-mail: olikh@univ.kiev.ua*

Submitted October 2, 2008; accepted for publication November 20, 2008

**Abstract**—Using the method of differential coefficients of current–voltage characteristics, deep levels in the *Cz*-Si *p–n* structures are studied under the ultrasonic loading conditions (longitudinal waves of a frequency of 4–26 MHz and intensity as high as 0.6 W/cm$^2$). The levels with thermal activation energy of 0.44, 0.40, 0.37, 0.48, and 0.46 eV are revealed. It is assumed that these levels are associated with the *E* center, bistable $B_SO_{2i}$ complex, and interstitial atoms captured by dislocation loops, respectively. It is established that ultrasound induces an increase in the contribution to the recombination processes of shallower levels and a decrease in activation energy of defects. The possibility of acoustoinduced reversible reconstruction of the configuration of the $B_SO_{2i}$ complex is analyzed.

PACS numbers: 43.35.Ty, 71.55.Cn, 61.72.Ji

**DOI:** 10.1134/S1063782609060116

## 1. INTRODUCTION

Methods of nonequilibrium modification of the defect–impurity subsystem with the purpose of obtaining new characteristics and properties of semiconductor crystals, structures, or devices, and the methods of the so-called "defect engineering", cause an increasingly great interest [1]. This is caused by the prospects for designing the component base of solid-state electronics of a new generation due to the controlled formation of active centers or nanoclusters using these methods. Undoubtedly, leaders in this field are the radiation methods; see, for example, [2, 3]. However, interesting results are also obtained with the study of alternative methods of affecting the defect structure of semiconductors, specifically, using ultrasonic waves for these purposes [4–8]. For example, it is shown that ultrasonic treatment stimulates regrouping of the defects [4], the decomposition [5] and formation [6] of various complexes, the formation of nanoparticles in the semiconductor bulk [7], and the variation in the concentration of defect centers at the oxide–semiconductor interface [8]. However, it should be noted that a rigorous theory for the interaction of the ultrasound with the defects, especially for low-dislocation crystals such as silicon, is absent. In connection with this, data on the effect of acoustic waves on the electrical activity of defects can be very useful.

In this article, we present the results of the experimental study of the effect of ultrasound on the energy location in the band gap and recombination activity of electron states associated with the defects in silicon *p–n* structures. It should be noted that the overwhelming majority of existing publications in this field are devoted to the study of variations in the properties of semiconductors as a result of ultrasonic treatment, i.e., to the irreversible residual effects of the acoustic influence. This article describes the variations appearing during the propagation of the ultrasonic wave in the crystal, which vanish after finishing the effect of elastic vibrations, i.e., the objects of examination are the reversible dynamic effects.

## 2. SAMPLES AND MEASUREMENT PROCEDURES

The samples for the studies (of the area of about 1 cm$^2$) were cut from the *p–n* structure (solar cell) of diameter 100 mm, the samples were cut from both the central part (we will further denote these samples as SC1) and from the region near the wafer's edge (SC2). This selection is caused by the fact that the defect distribution over the area of the semiconductor wafer is nonuniform and, consequently, we can expect distinction in the effect of ultrasound. The structure consisted of the *Cz*-*p*-Si substrate doped with boron ($p = 1.25 \times 10^{15}$ cm$^{-3}$) 300 μm thick. On the structure's surface, the layer with electron conductivity ($n \approx 10^{19}$ cm$^{-3}$, thickness of ~0.5 μm) was formed via implantation of phosphorus ions. Aluminum contacts were formed on the surface of this solar cell: the continuous contact on the *p* region and semitransparent contact on the *n* region.

The parameters of deep levels were determined via the analysis of current–voltage (*I–V*) characteristics according to the procedure suggested in [9]. Notably, the amount of peaks in the $\partial\beta/\partial U = f(U)$ dependences (where $\beta$ is the differential index of the slope of the $I$–$V$ characteristic, $\beta = (qI/k_BT)(\partial I/\partial U)^{-1}$, $q$ is the elementary charge, $I$ is the current passing across the $p$–$n$ structure, $U$ is the direct bias voltage, $T$ is temperature, and $k_B$ is the Boltzmann constant) corresponds to the number of various types of deep levels in the band gap of the semiconductor, which are effectively involved in the carrier recombination. In this case, the energy of thermal activation of the deep level $E_C - E_t^i$ is determined by the abscissa of the corresponding peak $U_0^i$:

$$E_C - E_t^i \approx (E_g - qU_0^i)/2, \qquad (1)$$

where $E_g$ is the band gap and $E_C$ is the energy location of the conduction band's bottom. Formula (1) is accurate to the systematic error $\delta$ depending on the material and the ratio of capture coefficients of electrons and holes $c_n/c_p$ for this center [9]; the performed estimations show that for Si at room temperature and $c_n/c_p = 10$, $\delta \approx 0.02$ eV. The amplitude of each maximum is determined by the contribution of one or another center to the carrier recombination [9]. We used the following procedure. The measured $I$–$V$ characteristic was corrected making allowance for the shunting resistance $R_{SH}$ [10], and the dependence $\partial\beta/\partial U = f(U)$ was constructed on its basis. This dependence was further approximated by the sum of the Gaussian curves, the number of which was determined by the number of the peaks. Based on thus found values of $U_0^i$, the values of $E_C - E_t^i$ for each deep level were calculated using formula (1). In this case, the relative contributions of each of the peaks $\eta_i$ to the total area were also evaluated ($\eta_i = S_i/S_\Sigma$, where $S_i$ is the area under the $i$th peak and $S_\Sigma$ is the total area under the entire curve). Further, the value of $\eta_i$ was considered as the index of the specific contribution of each of the deep levels to the total recombination.

The samples were placed into a special chamber, and longitudinal waves (with frequency $f_{US}$ equal to 4.1, 8.0, 13.6, and 26.1 MHz, respectively) were sequentially excited in them using replaceable piezotransformers. Since irreversible variations can already take place in the subsystem of defects of silicon under the intensity of acoustic loading $W_{US} > 1$ W/cm$^2$ [5, 6], the waves with $W_{US} < 0.6$ W/cm$^2$ were excited in our experiments. This corresponded to the strain in the sound wave $\varepsilon_{US} = \sqrt{2W_{US}/\rho v_{US}^3} < 3 \times 10^{-6}$, where $\rho$ is the density of silicon and $v_{US}$ is the velocity of sound. Note that the chamber design provided both screening of the piezotransducer and electrical isolation of measurement processes of the $I$–$V$ characteristics and excitation of ultrasound. As a consequence, penetration of the piezoelectric field into the sample was excluded. Therefore, all below-described effects can be determined only by the alternating-sign deformation. The experiments were performed at room temperature, and the sample temperature was controlled using a copper–constantan differential thermocouple. It is established that under ultrasonic loading, the sample temperature somewhat increased. However, heating did not exceed 20°C at maximum values of $W_{US}$.

The measurements of the $I$–$V$ characteristics were performed under the conditions of sequentially established temperatures: (i) before the ultrasonic loading of the sample; (ii) in 20–30 min after switching on the ultrasound; and (iii) in 20–30 min after completion of the ultrasonic loading. The temperature of the sample, which it had during the ultrasonic loading, was held using additional heating in last case. In the first and third cases, the obtained results almost coincided, which confirms the reversible character of acoustically induced phenomena at various values of $f_{US}$ and $W_{US}$.

## 3. EXPERIMENTAL RESULTS

Figure 3a represents the starting experimental dependence $\partial\beta/\partial U$ for the SC1 sample. Three peaks are observed in it, which according to [9] indicates the presence of three types of the levels determining the generation–recombination processes during the current passage. We will further denote these levels as $E1$, $E2$, and $E3$. The abscissas of the peaks $U_0^1$, $U_0^2$, and $U_0^3$ are 0.14, 0.21, and 0.28, respectively. The calculations by formula (1) showed that $E_C - E_t$ for the levels $E1$, $E2$, and $E3$ are 0.48, 0.44, and 0.40, respectively (see Table 1). It is evident from the diagram presented in Fig. 1a that, in the absence of ultrasound, the deepest level introduces the maximum contribution to recombination.

In the course of ultrasonic loading, the pattern of the peaks changes (see Figs. 1b, 1c). In particular, the ratios of the peak areas (contributions to recombination of various deep levels) vary, the shift of the location of the peaks (variation in the activation energy of deep levels) takes place, and the number of the peaks changes (new deep levels emerge). Generalizing the obtained data, we can make the following conclusions. (i) As $W_{US}$ increases, the role of the levels located nearer to the conduction band's bottom increases; the dependences of indices of the relative contribution of the levels on the strain are very close to linear ($\eta_i \propto \varepsilon_{US}$) (see Fig. 2). In addition, such acoustooptic variations proceed more effectively as the ultrasound frequency increases. (ii) Upon exceeding the threshold value $W_{US} \approx 0.10$ W/cm$^2$ (irrespective of the frequency), the signal from one more deep level denoted by us as $E4$, for which $E_C - E_t = 0.37$ eV, is observed. This is the shallowest of the levels observed by us, and its contribution to recombination also increases as

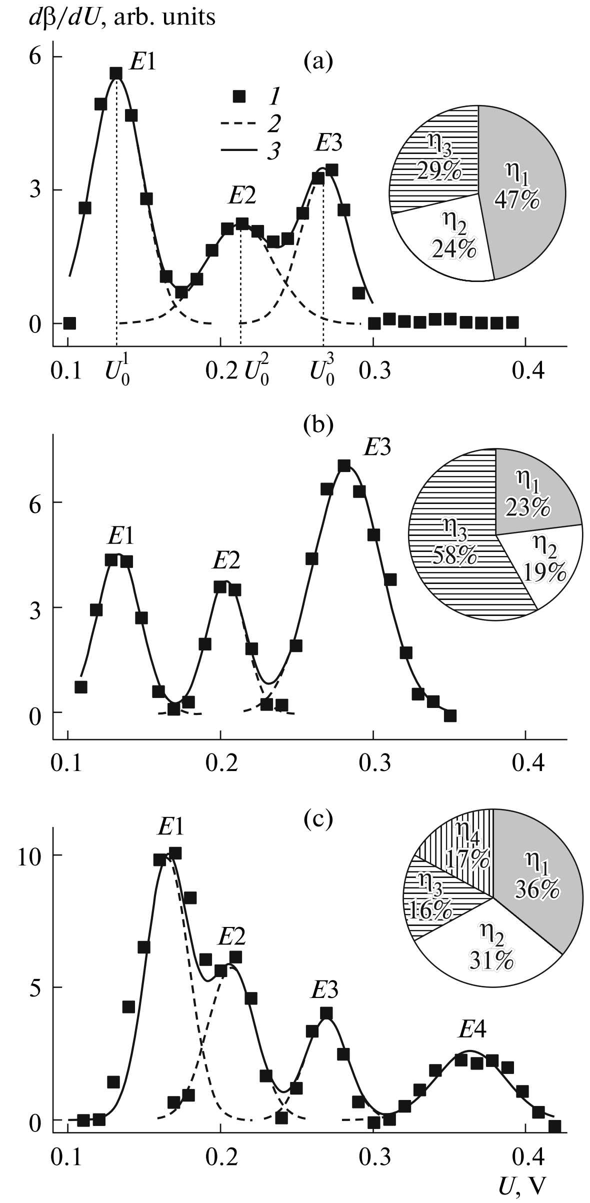


**Fig. 1.** Dependence of the derivative of the differential index for the slope of the *I–V* characteristic. The SC1 sample: (a) without the ultrasonic loading, (b) under the ultrasonic loading ($f_{US}$ = 26.1 MHz, $W_{US}$ = 0.10 W/cm$^2$), and (c) under the ultrasonic loading (4.1 MHz, 0.25 W/cm$^2$). (*1*) The points obtained after differentiating the experimental *I–V* characteristics; (*2*) Gaussian curves, by which the maxima were approximated; and (*3*) the sum of all Gaussians. The diagrams of relative contributions $\eta_i$ of each of the peaks are represented near the curves to the right.

$W_{US}$ increases. (iii) At $W_{US} > 0.3$ W/cm$^2$, an insignificant shift of the levels *E*1 and *E*2 nearer to the conduction band's bottom by 0.010–0.015 eV is observed (see Table 1).

The results obtained for SC2 samples are presented in Fig. 3 and Table 2. It is evident that, in this case, the

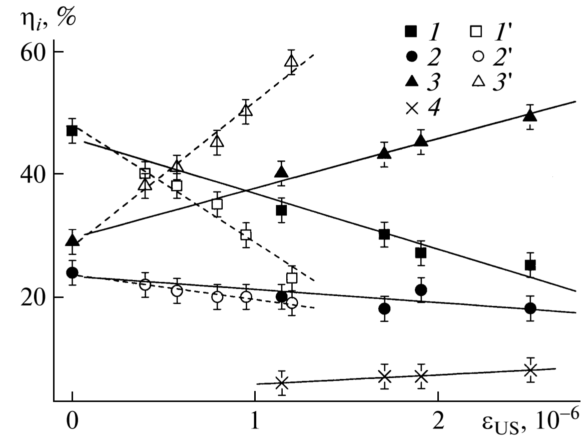


**Fig. 2.** Dependence of specific contributions to the total recombination of separate levels *E*1 (curves *1* and *1'*), *E*2 (*2* and *2'*), *E*3 (*3* and *3'*), and *E*4 (*4*) on the value of the relative vibrational deformation under ultrasonic loading with $f_{US}$ = 4.1 MHz (curves *1–4*) and $f_{US}$ = 26.1 MHz (*1'–3'*). The points are obtained after the analysis of the experimental *I–V* characteristics, and the lines correspond to their linear approximation.

pattern is more complex than for SC1; in particular, even without ultrasonic loading, the *E*4 peak is observed and, in addition, one more peak denoted as *E*11, which is associated with the level $E_C - E_t$ = 0.46 eV, is observed. In general, the character of acoustically induced variations in SC2 samples resembles that observed in SC1 samples, namely, an increase in the specific contribution to recombination of the levels located nearer to $E_C$ takes place, the effect increases as $f_{US}$ increases, and a decrease in the activation energy of deep levels *E*2, *E*3, and *E*4 by 0.010–0.015 eV is observed for ultrasonic loading of sufficient intensity (see Table 1). However, the efficiency of ultrasonic loading is somewhat lower compared with SC1 samples.

## 4. DISCUSSION

On the basis of the obtained values of $E_C - E_t$ and known published data, let us attribute the concrete defects to the levels *E*1–*E*4. It seems likely that the *E* center corresponds to the *E*2 level (the pair vacancy–phosphorus), for which $E_C - E_t$ = 0.43–0.44 eV [11, 12]. Indeed, in the samples under study, it is phosphorus which is the doping impurity in the *n*-type layer; it is also known that this center effectively affects the recombination processes [11].

As for the *E*3 level, it is our opinion that it corresponds to the $B_SO_{2i}$ complex, or the defect, which consists of the substitutional boron and dimer. Indeed, (I) the location of the level corresponding to $B_SO_{2i}$, $E_C - E_t$ = 0.40–0.41 eV [13, 14], which coincides with the data obtained for *E*3; (II) $B_SO_{2i}$ belongs to the main recombination centers in *Cz*-Si:B [13], which is the substrate material of the structures under study;

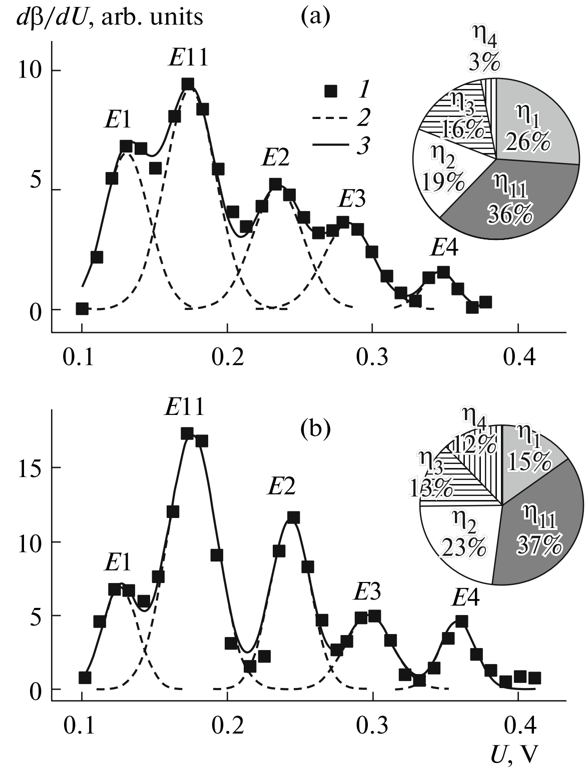


**Fig. 3.** The same as in Fig. 1. The SC2 sample: (a) without ultrasonic loading and (b) with ultrasonic loading (4.1 MHz, 0.60 W/cm$^2$).

and (III) the $B_SO_{2i}$ concentration increases under illumination or injection of minority carriers due to an increase in mobility of the $O_i$–$O_i$ complex and its subsequent capture by the boron ion [13]. In our case, under the monochromatic illumination with a wavelength of 900 nm, an increase in recombination of the $E3$ center is observed ($\eta_3$ varies from 25 to 29% for SC1 and from 7 to 16% for SC2). This indicates an increase in the concentration of corresponding defects.

Metastability of defects is a very important and positive factor for the manifestation of acoustodynamic effects in semiconductors [15]. It is the charge-dependent configuration bistability, which is characteristic of $B_SO_{2i}$ [13, 16]: the defect can be found either in the $B_SO_{2i}^{sq}$ configuration (more probable for the single positively charged state) or in the $B_SO_{2i}^{st}$ configuration (more probable for the neutral state). The $E_C -$ 0.40 eV level is referred to as $B_SO_{2i}^{sq}$ [13]. It is our opinion that it is the intensification of the recharge process of the $B_SO_{2i}$ complex under the effect of ultrasound that manifests itself in an increase in the contribution of the $E3$ level in recombination processes, and also leads to the transition $B_SO_{2i}^{sq} \longrightarrow B_SO_{2i}^{st}$ in a fraction of defects. Such a transition is associated with overcoming the potential barrier [16]; therefore, it becomes effective only after exceeding the threshold value by $W_{US}$. In connection with this, let us note that one of the components of the $B_SO_{2i}$ complex, precisely the dimer, as a result of recharge, reconstructs similarly $O_{2i}^{sq} \longrightarrow O_{2i}^{st}$ [13, 16] (diffusion by the Bourgoin mechanism takes place). We assume that the emergence of the peak $E4$ under the acoustoinduced transition $B_SO_{2i}^{sq} \longrightarrow B_SO_{2i}^{st}$ indicates that the found levels $E3$ and $E4$ refer to the same defect $B_SO_{2i}$ but is situated in different configurations. In connection with this, we consider the sum $\eta_3 + \eta_4$ (see Table 2) assuming the levels $E3$ and $E4$ as two states of $B_SO_{2i}$. From here, the conclusion follows that the contribution to recombi-

**Table 1.** Comparison of the obtained values of the activation energy of deep levels with the published data

| Obtained results | | | | | Published data | | |
|---|---|---|---|---|---|---|---|
| Level | $E_C - E_t^{**}$, eV | | | | $E_C - E_t$, eV | defect type | source |
| | SC1 | | SC2 | | | | |
| | without | with* | without | with* | | | |
| $E1$ | 0.48 | 0.47 | 0.48 | 0.48 | 0.475 | C–O–$V_2$ | [17] |
| $E11$ | – | – | 0.46 | 0.46 | 0.44–0.48 | $I$ | [20] |
| $E2$ | 0.44 | 0.425 | 0.43 | 0.42 | 0.43–0.44 | $V$–Ps ($E$ center) | [11, 12] |
| $E3$ | 0.40 | 0.40 | 0.40 | 0.39 | 0.40 | $BsO_{2i}^{sq}$ | [13] |
| | | | | | ? | $BsO_{2i}^{st}$ | |
| $E4$ | 0.37 | 0.37 | 0.37 | 0.355 | 0.37 | $B_i$ | [17] |

* Parameters of ultrasonic loading: $f_{US} = 4.1$ MHz, $W_{US} = 0.43$ W/cm$^2$ (for SC1) and $W_{US} = 0.60$ W/cm$^2$ (for SC2).
** Random error determining $E_C - E_t$ is 0.01 eV.

**Table 2.** Relative contribution of deep levels to recombination processes for SC2 under various modes of ultrasonic loading

| $f_{US}$, MHz | $\varepsilon_{US}$, $10^{-6}$ | $\eta_1$, % | $\eta_{11}$, % | $\eta_1 + \eta_{11}$, % | $\eta_2$, % | $\eta_3$, % | $\eta_4$, % | $\eta_3 + \eta_4$, % |
|---|---|---|---|---|---|---|---|---|
| – | – | 26 | 36 | 62 | 19 | 16 | 3 | 19 |
| 4.1 | 1.6 | 19 | 43 | 62 | 14 | 18 | 6 | 24 |
| | 2.1 | 17 | 40 | 57 | 19 | 17 | 7 | 24 |
| | 2.5 | 13 | 42 | 55 | 22 | 15 | 8 | 23 |
| | 3.0 | 15 | 37 | 52 | 23 | 13 | 12 | 25 |
| 13.6 | 0.5 | 18 | 36 | 54 | 18 | 20 | 8 | 28 |
| | 1.0 | 10 | 37 | 47 | 19 | 26 | 8 | 32 |
| | 1.5 | 4 | 44 | 48 | 19 | 26 | 7 | 33 |

Note: Accuracy in determining the energy of the relative contribution to recombination is 2%.

nation of the $B_SO_{2i}$ complex in general increases under the effect of elastic vibrations.

The transition of defects to an unstable state under the effect of ultrasound was also observed previously [6, 15]. Our results indicate that the effect increases as the frequency of the acoustic waves increases.

However, it is known [17] that the state $E_C - E_t$ = 0.37 eV can correspond to the acceptor level of the interstitial boron atom $B_i$. In connection with this, we can suggest another mechanism of acoustically induced emergence of the level $E4$. Specifically, liberation of self-interstitials $I$ captured by dislocation loops near the $p$–$n$ junction takes place (considerable amount of $I$ defects and dislocations is easily explainable by the ion implantation used to fabricate the structure). After that, the diffusion of $I$ inside the $p$ region, where they force out the B atoms from the lattice sites by the Watkins mechanism, takes place. However, (i) under such an approach, it is rather difficult to interpret the disappearance of the signal associated with $E4$ after ultrasound loading; (ii) $B_i$ is the center with negative correlation energy, and its donor level $E_C - E_t$ = 0.13 eV [17] is closer to $E_C$; therefore, it is almost improbable to observe the acceptor level in $p$-Si. As a consequence, this mechanism seems to be improbable.

Let us now refer to the level $E1$. Its activation energy of 0.48 eV is very close to the location of the level of the complex C–O–$V_2$—$E_C - E_t$ = 0.47 eV [18]. However, this center was observed in $n$-Si irradiated either with electrons or with $\gamma$-ray photons [18], and we believe that its emergence in the structures under study is unlikely. It is our opinion that $E1$ is associated with interstitial atoms (intrinsic or impurity), which are captured by dislocations—these are the defects which are the effective recombination centers [19]. For example, in [20], it is assumed that the defect $I$ corresponds to the level $E_C - E_t$ = 0.44–0.48 eV. However, in general, the energy location of the levels of captured defects can differ from the values in the bulk [19]. A definite basis for such correlations emerges upon considering the results obtained for SC2. It is known that on the peripheral portions of semiconductor wafers, the defect concentration is higher than in the central part. In our case, this is indirectly indicated by a considerable decrease in shunting resistance in SC2 (~$2 \times 10^3$ Ω) compared with SC1 (~$2 \times 10^4$ Ω). Indeed, a decrease in $R_{SH}$ is usually associated with the presence of structural defects at the interface between the $p$- and $n$-type regions, with an increase in the impurity concentration, and with current processes over grain boundaries and dislocations [10, 21]. It is possible that the appreciably higher impurity concentration in SC2 captured by the dislocation loops leads to the fact that the two levels ($E1$ and $E11$) are observed in the range $E_C$ – (0.46–0.48) eV, the contribution of which to the recombination is substantially higher than in SC1 (see Figs. 1, 3). It is possible that levels $E1$ and $E11$ correspond to the same defect in different configurations, one of which is distorted because of the close arrangement of the dislocation loop. Consequently, their contribution to recombination processes can be also considered in total ($\eta_1 + \eta_{11}$, see Table 2). In addition, under the effect of ultrasound, the reconstruction $E1 \longrightarrow E11$ takes place; its efficiency increases as $f_{US}$ increases (Fig. 3, Table 1, ratio between $\eta_1$ and $\eta_{11}$).

The manifestation of $E4$ in the acoustically unperturbed SC2 sample can be also attributed to a high content of impurities: a high starting concentration of $B_SO_{2i}$ allows us to reveal level $E4$, and the ratio of concentrations $B_SO_{2i}^{st}$ and $B_SO_{2i}^{sq}$ as in SC1 is retained in this case. The lower efficiency of the acoustically induced increase in contribution to recombination processes of shallower levels for SC2 compared with SC1 can be caused by larger absorption of ultrasound by defects in the region of the $p$–$n$ junction. As a result, a considerable part of the introduced energy is consumed by the processes of the $E1 \longrightarrow E11$ type, while the acoustic vibrations of lower efficiency penetrate into the $p$-type region.

Let us also note that a decrease in the activation energy of deep levels by 0.010–0.015 eV during the ultrasonic loading of sufficient intensity cannot be accounted for by acoustically induced heating of the sample by ≤20 K since the characteristic value of the temperature coefficients of varying the location of the levels of impurity centers in the band gap is $\sim 10^{-4}$ eV/K. This result is indicative of the modification of the electron structure of the complexes $P_S$–$V$ and $B_SO_{2i}$ due to the interaction with nonequilibrium phonons excited by ultrasound.

Therefore, the results presented in this article confirm the practical prospects of dynamic acoustic control over the properties of semiconductors and characteristics of devices on their basis. It should be noted that the nonequilibrium state of defects (in our case, recombination centers), which emerges with the emergence of nonequilibrium charge carriers, serves as an important factor of increasing the efficiency of acoustodefect interaction in general. This is the situation, in which the additional vibrational energy of the external ultrasound becomes a more effective means of the control over the characteristics of the device in general. Undoubtedly, the questions of acoustically induced transformations of the structure, configuration, and charged state of defects in semiconductors require the further studies.

## 5. CONCLUSIONS

In this study, for the first time in the dynamic mode, the behavior of deep levels in silicon $p$–$n$ structures during ultrasound vibrations was studied. It was found that, as the amplitude of the ultrasound increases, the contribution to the recombination processes of shallower levels increases, and this process almost linearly depends on the strain in the elastic wave. A decrease in the energy of thermal activation of defects is also observed, and the efficiency of such processes increases as the frequency of acoustic vibrations is increased. The obtained results are interpreted qualitatively in the context of the model of acoustically induced reconstruction of impurity defect complexes.

## ACKNOWLEDGMENTS

I thank V. P. Kostylev (Institute of Semiconductor Physics, National Academy of Sciences of Ukraine) for letting us have the samples for measurements.

This study was supported by the Foundation of the Ukrainian Scientific and Research Center, project no. 3555.

## REFERENCES

1. L. S. Smirnov, Fiz. Tekh. Poluprovodn. **35**, 1029 (2001) [Semiconductors **35**, 985 (2001)].
2. V. V. Kozlovskii, V. A. Kozlov, and V. N. Lomasov, Fiz. Tekh. Poluprovodn. **34**, 129 (2000) [Semiconductors **34**, 123 (2000)].
3. A. R. Chelyadinskii and F. F. Komarov, Usp. Fiz. Nauk **173**, 813 (2003) [Phys. Usp. **46**, 789 (2003)].
4. E. M. Zobov, M. E. Zobov, F. S. Gabibov, I. K. Kamilov, F. I. Manyakhin, and E. K. Naimi, Fiz. Tekh. Poluprovodn. **42**, 282 (2008) [Semiconductors **42**, 277 (2008)].
5. A. A. Podolyan and V. I. Khivrich, Pis'ma Zh. Tekh. Fiz. **31** (10), 11 (2005) [Tech. Phys. Lett. **31**, 408 (2005)].
6. Ya. M. Olikh, N. D. Timochko, and A. P. Dolgolenko, Pis'ma Zh. Tekh. Fiz. **32** (13), 67 (2006) [Tech. Phys. Lett. **32**, 586 (2006)].
7. A. Romanyuk, V. Spassov, and V. Melnik, J. Appl. Phys. **99**, 034314 (2006).
8. P. B. Parchinskii, S. I. Vlasov, and L. G. Ligai, Fiz. Tekh. Poluprovodn. **40**, 829 (2006) [Semiconductors **40**, 808 (2006)].
9. S. V. Bulyarskii, M. O. Vorob'ev, N. S. Grushko, and A. V. Lakalin, Pis'ma Zh. Tekh. Fiz. **25** (5), 22 (1999) [Tech. Phys. Lett. **25**, 176 (1999)].
10. V. V. Serdyuk, *Physics of Solar Cells* (Logos, Odessa, 1994) [in Russian].
11. P. V. Kuchinskii and V. M. Lomako, Solid State Electron. **29**, 1041 (1986).
12. S. Zh. Karazhanov, Semicond. Sci. Technol. **16**, 276 (2001).
13. J. Schmidt, K. Bothe, D. Macdonald, J. Adey, R. Jones, and D. W. Palmer, J. Mater. Res. **21** (1), 5 (2006).
14. S. Rein and S. W. Glunz, Appl. Phys. Lett. **82**, 1054 (2003).
15. O. Ya. Olikh and I. V. Ostrovskii, Fiz. Tverd. Tela **44**, 1198 (2002) [Phys. Solid State **44**, 1249 (2002)].
16. J. Adey, R. Jones, D. W. Palmer, P. R. Briddon, and S. Oberg, Phys. Rev. Lett. **93**, 055504 (2004).
17. R. D. Harris, J. L. Newton, and G. D. Watkins, Phys. Rev. B **36**, 1094 (1987).
18. P. F. Lugakov, V. D. Tkachev, and V. V. Shusha, Fiz. Tekh. Poluprovodn. **13**, 875 (1979) [Sov. Phys. Semicond. **13**, 514 (1979)].
19. V. Kveder, M. Kittler, and W. Schroter, Phys. Rev. B **63**, 115208 (2001).
20. V. V. Luk'yanitsa, Fiz. Tekh. Poluprovodn. **37**, 422 (2003) [Semiconductors **37**, 404 (2003)].
21. V. I. Gaman, *Physics of Semiconductor Devices* (NLT, Tomsk, 2000) [in Russian].

*Translated by N. Korovin*